Muscle-specific, liver-detargeted adeno-associated virus gene therapy rescues Pompe phenotype in adult and neonate Gaa−/− mice

P. Sellier, P. Vidal, B. Bertin, E. Gicquel, E Bertil-froidevaux, C. Georger, L. van Wittenberghe, A. Miranda, N. Daniele, Isabelle Richard, et al.

Received: 21 December 2022 | Revised: 17 March 2023 | Accepted: 11 May 2023

DOI: 10.1002/jimd.12625

ORIGINAL ARTICLE

JIMD SSIEM WILEY

Muscle-specific, liver-detargeted adeno-associated virus gene therapy rescues Pompe phenotype in adult and neonate *Gaa*$^{-/-}$ mice

P. Sellier[1,2] | **P. Vidal**[1,2] | **B. Bertin**[1,2] | **E. Gicquel**[1,2] | **E. Bertil-Froidevaux**[2] | **C. Georger**[2] | **L. van Wittenberghe**[2] | **A. Miranda**[2] | **N. Daniele**[2] | **I. Richard**[1,2] | **D. A. Gross**[1,2] | **F. Mingozzi**[1,2] | **F. Collaud**[1,2] | **G. Ronzitti**[1,2]

[1]Université Paris-Saclay, Univ Evry, Inserm, Genethon, Integrare Research Unit UMR_S951, Evry, France

[2]Genethon, Evry, France

Correspondence
G. Ronzitti, INSERM U951 "INTEGRARE," Genethon, Univ Evry, Université Paris-Saclay, 1bis rue De l'Internationale 91000 Evry, France.
Email: gronzitti@genethon.fr

Present address
F. Mingozzi, Spark Therapeutics, Philadelphia, Pennsylvania, USA.

Funding information
Genethon and the French Muscular Dystrophy Association (AFM); SPARK Competitive Research Grant Program on Pompe disease

Communicating Editor: Nicola Brunetti-Pierri.

Abstract

Pompe disease (PD) is a neuromuscular disorder caused by acid α-glucosidase (GAA) deficiency. Reduced GAA activity leads to pathological glycogen accumulation in cardiac and skeletal muscles responsible for severe heart impairment, respiratory defects, and muscle weakness. Enzyme replacement therapy with recombinant human GAA (rhGAA) is the standard-of-care treatment for PD, however, its efficacy is limited due to poor uptake in muscle and the development of an immune response. Multiple clinical trials are ongoing in PD with adeno-associated virus (AAV) vectors based on liver- and muscle-targeting. Current gene therapy approaches are limited by liver proliferation, poor muscle targeting, and the potential immune response to the hGAA transgene. To generate a treatment tailored to infantile-onset PD, we took advantage of a novel AAV capsid able to increase skeletal muscle targeting compared to AAV9 while reducing liver overload. When combined with a liver-muscle tandem promoter (LiMP), and despite the extensive liver-detargeting, this vector had a limited immune response to the hGAA transgene. This combination of capsid and promoter with improved muscle expression and specificity allowed for glycogen clearance in cardiac and skeletal muscles of *Gaa*$^{-/-}$ adult mice. In neonate *Gaa*$^{-/-}$, complete rescue of glycogen content and muscle strength was observed 6 months after AAV vector injection. Our work highlights the importance of residual liver expression to control the immune response toward a potentially immunogenic transgene expressed in muscle. In conclusion, the demonstration of the efficacy of a muscle-specific AAV capsid-promoter combination for the full rescue of PD manifestation in both neonate and adult *Gaa*$^{-/-}$ provides a potential therapeutic avenue for the infantile-onset form of this devastating disease.

KEYWORDS
AAV, dual promoter, lysosomal storage disorders, neuromuscular diseases, Pompe disease

1 | INTRODUCTION

Glycogen storage disease type II, also named Pompe disease (PD) (GSD-II, OMIM#232300) is an autosomal recessive disorder (1/40000 births) caused by mutations in the gene encoding for acid α-glucosidase (GAA). This enzyme plays a central role in the degradation of glycogen to glucose in lysosomes. GAA deficiency leads to a pathological glycogen accumulation in lysosomes and the consequent autophagic impairment in all the tissues of the body. Heart and skeletal muscles are particularly affected in PD patients with cardiac insufficiency, muscles weakness, respiratory failure, and neurological damages being the major symptoms.[1] Enzyme replacement therapy (ERT) with recombinant human GAA (rhGAA) is the current treatment for PD. Two main forms of PD are distinguished: the infantile-onset (IOPD) and the late-onset (LOPD).

In LOPD patients, where the later onset is due to residual GAA activity (>1%), one of the major difficulties is the demonstration of the efficacy of ERT or other treatments due to the slow disease progression. However, a recent meta-data analysis conducted on multiple clinical studies indicated significantly improved walking distance and a stabilization of the respiratory function and muscle strength after treatment with ERT.[2] In LOPD, immune reactions to rhGAA may have a potential impact on the ERT efficacy, in particular in the presence of high antibody titers.[3,4]

IODP patients have no GAA activity (<1%) and, without treatment, they die in the first years of age. ERT in IOPD patients showed increased ventilator-free survival and improved cardiac function.[5–7] Long-term evaluation of ERT efficacy clearly indicated that, despite sustained cardiac benefits, both respiratory and muscle functions declined with aging.[8–13] Importantly, this decline was also observed in patients positive for cross-reactive immune material (CRIM+) treated from early age. In CRIM- patients, that is, those patients without GAA expression, immune responses to rhGAA greatly reduce ERT efficacy.[5,14–16]

In the last years, a multitude of gene therapy approaches were developed for PD, and some of them reached either the preclinical or the clinical phase (recently reviewed in Reference 17). Both ex vivo, with genetically modified CD34+ cells, and in vivo gene therapy approaches were pursued. In vivo gene therapy with AAV vectors is mainly based on two distinct approaches, targeting either the liver or the muscle. The liver approach is based on early findings that demonstrated that liver-targeted expression of hGAA improved glycogen accumulation in muscle.[18–20] The efficacy of this strategy was further improved by increasing the levels of GAA secretion by hepatocytes or combining gene therapy with small molecules[21–23] and recently tested in the clinic in two distinct trials (NCT03533673 and NCT04093349). Preclinical research in animal models of the disease has clearly demonstrated a dose advantage for the liver as well as a robust immune tolerance induced when hepatocytes were specifically targeted.[21,24,25] However, one important limitation of liver gene transfer is the high replication rate of hepatocytes during liver growth, which is likely to result in transgene dilution and loss of efficacy over time when the treatment is applied in young individuals.[26]

On the other hand, the use of muscle-specific expression cassettes showed efficient expression of the hGAA transgene in relevant organs as well as reduced glycogen accumulation and significant improvement of muscle function in mouse models of PD.[27–37] Limitations associated to this approach include the need for high doses of vector to efficiently target muscle in humans (> 10^{14} vg/kg),[38–40] the risk of liver-related toxicity due to capsid off-targeting[41] and the potential anti-hGAA antibody formation in particular in CRIM-patients.[27,42] Recently, a liver-muscle tandem promoter (LiMP) was proposed to control the immunogenicity of hGAA.[24] The use of LiMP to express a secretable form of hGAA with AAV9 resulted in the complete correction of glycogen accumulation in neonate *Gaa*$^{-/-}$ mice, with total glycogen clearance, at the dose of 6×10^{12} vg/kg.[24] However, the use of AAV9, a liver-tropic capsid, to express secretable hGAA in both liver and muscle, complicates the evaluation of the contribution of the two tissues to efficacy and immune response control.

In the present study, we took advantage of a recently developed muscle targeting capsid (AAV-MT) and of the improved muscle-specific transgene expression of the LiMP to express the native form of hGAA specifically in muscle. We combined the advantageous biodistribution profile of this AAV capsid with the LiMP. This promoter, aside a robust expression in liver, has the main advantage of having a robust expression in muscle, strikingly higher than the parental SpC5-12 promoter. The use of such a strong promoter in combination with the liver detargeting properties of AAV-MT allowed us to achieve efficient muscle targeting while expressing the transgene in liver at levels that enabled immune tolerance without

overloading the tissue. Comparison with a similar construct expressed by AAV9 indicated a superior efficacy of the muscle-specific approach despite a complete lack of liver expression obtained by AAV-MT in adult *Gaa*$^{-/-}$ mice. Complete liver detargeting by AAV-MT led to increased humoral immune response to hGAA, while very low liver targeting, achieved with higher doses of the same capsid, was sufficient to reduce this immune response. Treatment of neonate *Gaa*$^{-/-}$ mice with the same approach confirmed the efficacy of specific muscle targeting in PD.

2 | RESULTS

2.1 | AAV-MT mediated gene transfer results in superior clearance of glycogen in skeletal muscle of adult *Gaa*$^{-/-}$ mice

Simultaneous expression of an engineered hGAA (Δ8-hGAAco) in liver and muscle with an AAV9 vector under the transcriptional control of the LiMP has shown efficacy in *Gaa*$^{-/-}$ mice.[24] To evaluate the contribution of muscle-specific hGAA expression by LiMP, we exploited the muscle-targeting specificity achieved by grafting RGD-containing peptides[43–45] in an AAV capsid with enhanced liver detargeting.[46] We cloned the RGDLGLS peptide (P1) between amino acids 586 and 602 of a new AAV capsid generated by the combination of AAV9 and AAV-RH74 (Figure S1A) following a previously described method.[45] The resulting capsid, named AAV-MT (for Muscle Transduction,[47]), was used to express the native form of codon-optimized (co), human GAA (hGAAco)[21] under the transcriptional control of the LiMP (Figure S1B). The native secretion-peptide of hGAA was used to specifically evaluate the advantage of improved muscle targeting with AAV-MT by reducing circulating GAA derived from residual liver expression and avoid cross-correction.

In a first experiment performed in four-month-old *Gaa*$^{-/-}$ mice, we compared the short-term efficacy of an AAV-MT vector expressing hGAAco under the control of the LiMP, to the efficacy obtained when the same transgene was expressed by AAV9 either using SpC5-12, a known muscle promoter, or LiMP (Figure 1A). One month after injection of the three vectors at the dose of 3×10^{12} vg/kg, in line with what was previously described,[24] we observed a marked improvement of GAA activity in heart and in different muscle groups in mice treated with AAV9-LiMP, compared to mice treated with AAV9-SpC5-12 (Figure 1B). When compared to AAV9, the combination of AAV-MT capsid with the LiMP, while resulting in similar heart transduction, led to a striking increase in skeletal muscle targeting, as shown by GAA activity (Figure 1B) and vector genome copy number (VGCN) analysis (Figure S2A). Increased GAA activity was invariably associated with improved glycogen clearance (Figure 1C), supporting the potential of AAV-MT in muscle targeting and rescue of phenotype in *Gaa*$^{-/-}$ mice. One exception was represented by the diaphragm, where, despite similar VGCN among the three vectors, GAA activity was increased in *Gaa*$^{-/-}$ mice treated with AAV-MT. This apparent discrepancy may be due to the presence of unprocessed viral particles at one-month post-injection or to the differential targeting of cell populating the diaphragm by the two vectors.

As expected, higher GAA activity was observed in the liver of mice injected with AAV9-LiMP, whereas animals receiving AAV-MT with the same promoter showed lower hepatic GAA activity, comparable to that measured in animals injected with AAV9-SpC5-12 (Figure 1D). The extensive liver detargeting of the AAV-MT was also confirmed by the VGCN analysis in this tissue (Figure S2B). Given the central role of the liver in establishing peripheral tolerance to antigens expressed in muscle,[18,20,48,49] the increased muscle expression and the decreased liver targeting, achieved by the combination of AAV-MT capsid and LiMP, resulted in increased levels of circulating anti-hGAA antibodies measured three and 4 weeks after vector injection (Figure 1E). These data suggest that the use of AAV-MT combined with LiMP can improve glycogen clearance in *Gaa*$^{-/-}$ mice while reducing the dose and detargeting the liver.

To confirm the increased muscle targeting of this novel AAV-MT capsid compared to AAV9, and to assess its therapeutic potential and immunogenicity when combined with the LiMP, we extended the comparison at two different doses. For this purpose, four-month-old *Gaa*$^{-/-}$ mice were injected with the two vectors at 1×10^{12} or 3×10^{12} vg/kg and sacrificed 3 months later to compare vector efficacy (Figure 2A). At the lower dose, while GAA activity was similar in heart and diaphragm regardless of the treatment received by *Gaa*$^{-/-}$ mice, a tendency for higher GAA activity was observed in skeletal muscle of mice treated with AAV-MT vector (Figures 2B and S3A). In the two groups treated at the higher vector dose, a significantly higher GAA activity was measured in cardiac and skeletal muscles of AAV-MT injected animals (Figures 2B and S3A), also confirmed by GAA quantification by Western blot analysis in quadriceps and soleus (Figure 2C,D). Consistently, increased GAA protein and activity was associated to better glycogen clearance in skeletal muscle (Figure 2E). Treatment with AAV-MT-LiMP resulted in complete clearance of glycogen from heart and all the muscles tested at the dose of 3×10^{12} vg/kg (Figures 2E and S3B). Importantly, at this dose, AAV9-LiMP was not able to clear glycogen from diaphragm and soleus. At the lower dose, 1×10^{12} vg/kg, AAV-MT showed a significantly better efficacy in

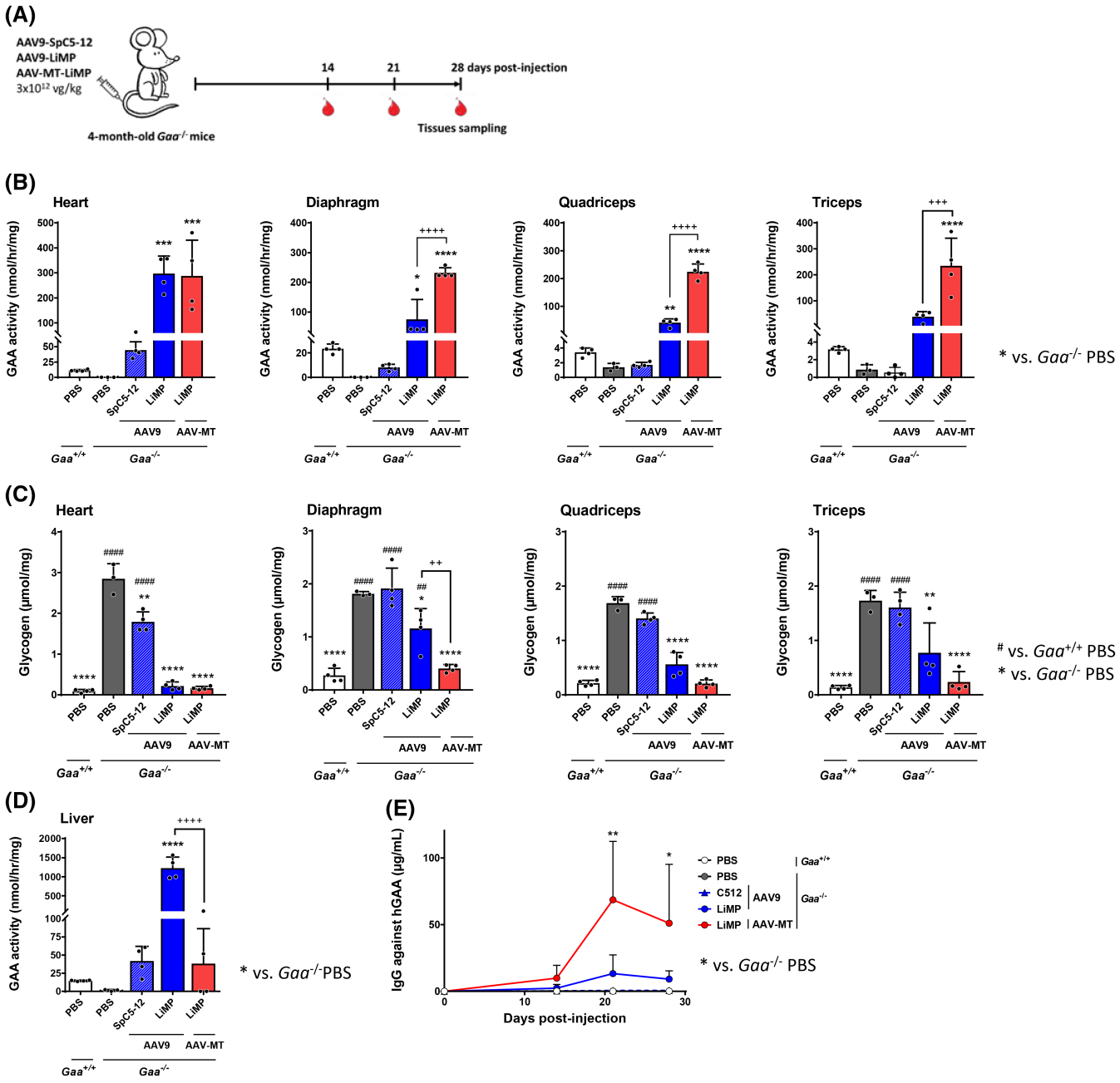

FIGURE 1 Combination of AAV-MT with LiMP leads to increased hGAA expression and a trend toward improved glycogen clearance in adult *Gaa*$^{-/-}$ mice at short-term. (A) Experimental design. 4-month-old *Gaa*$^{-/-}$ mice received a single injection of AAV9-SpC5-12-hGAAco, AAV9-LiMP-hGAAco or AAV-MT-LiMP-hGAAco at 3×10^{12} vg/kg ($n = 4$ per group). PBS-injected *Gaa*$^{+/+}$ ($n = 4$) and *Gaa*$^{-/-}$ ($n = 4$) mice were used as controls. Red symbols indicate the timing of blood collection in all cohorts. (B) Analysis of GAA activity and (C) glycogen content in heart and muscle, 1 month after vector injection. (D) GAA activity in liver. (E) Circulating anti-hGAA IgG measured over time. Data are shown as mean ± SD. Statistical analysis; (B–E) One-way ANOVA with Tukey post hoc; * and $^{\#}p < 0.05$, ** and $^{\#\#}p < 0.01$, *** and $^{+++}p < 0.001$, ****, $^{++++}$ and $^{\#\#\#\#}p < 0.0001$. Statistical significance was reported as: $^{\#}$ versus *Gaa*$^{+/+}$, * versus *Gaa*$^{-/-}$, and with $^{+}$ versus the indicated group.

glycogen clearance in quadriceps, with a tendency toward a better clearance in EDL and triceps (Figures 2E and S3B). The higher muscle targeting of AAV-MT capsid was further confirmed by the tendency to achieve higher VGCNs measured in heart and triceps of *Gaa*$^{-/-}$ mice injected with this vector when compared to AAV9 (Figure S3C). Grip-strength assay performed 3 months after AAV injection showed a tendency for an increased muscle strength in all treated animals regardless of the AAV vector, although none of the groups reached a statistical significance, possibly due to the low number of mice used in this analysis (Figure S3D).

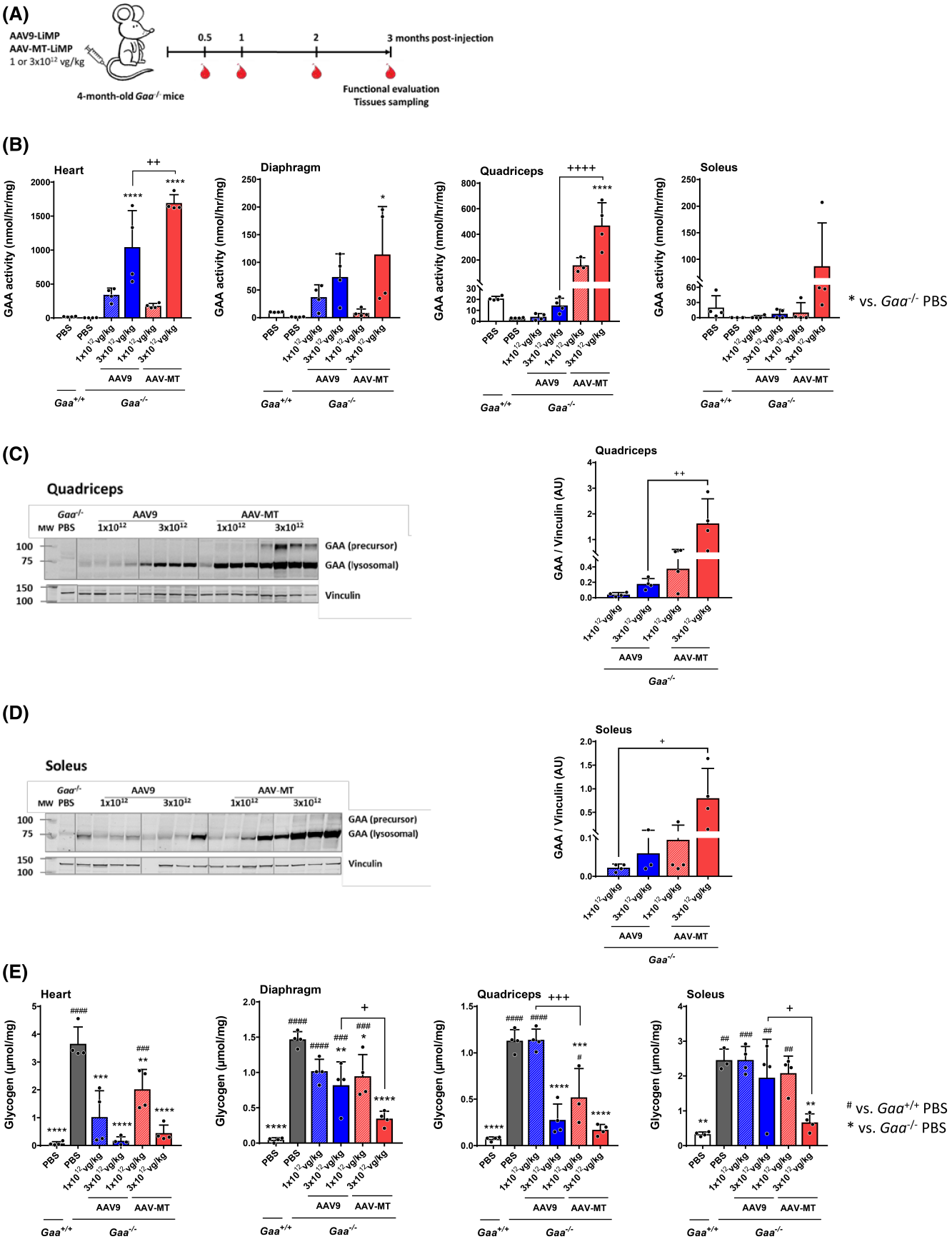

FIGURE 2 Legend on next page.

The insertion of the P1 peptide between amino acids 586 and 602 abolished the binding to heparan sulfate, central to liver targeting in rodents,[50] in an AAV capsid that showed already a pronounced liver de-targeting.[46] As expected, VGCN analysis in liver showed robust targeting with AAV9 and reduced copies per cell when the new capsid was used, regardless of the dose (Figure 3A). The combination of LiMP and AAV9 allowed for a robust expression of the transgene in liver, whereas with AAV-MT very low GAA activity levels were measured (Figure 3B). Western blot analysis confirmed the activity results with a strong hGAA band in AAV9-LiMP-injected $Gaa^{-/-}$ mice (Figure 3C). Importantly, $Gaa^{-/-}$ mice treated with AAV-MT-LiMP vector at the dose of 3×10^{12} vg/kg showed a faint band consistent with the size of mature hGAA protein, thus indicating some residual liver expression in this treatment group (Figure 3C). Circulating hGAA was relatively low across the different groups, possibly due to the use of the native form of hGAA,[21] although we were able to measure circulating hGAA by Western blot in animals treated with AAV9-LiMP (Figure 3D). These results confirm a strong, dose-dependent liver de-targeting by the AAV-MT.

AAV-mediated hepatocyte-specific expression of a transgene induces a strong peripheral tolerance to transgenes expressed in muscle.[18,20,48,49] Consistently, in our previous work, we demonstrated that combined expression of hGAA in liver and muscle with LiMP resulted in very low humoral immunity to hGAA in $Gaa^{-/-}$ mice, compared with a muscle-specific promoter.[24] To understand how liver detargeting by AAV-MT impacts the humoral response against the protein, we followed the anti-hGAA IgG levels over time through an ELISA test (Figure 3E). $Gaa^{-/-}$ mice treated with AAV9-LiMP showed a low and transient humoral immune response to hGAA that peaked at one-month post-injection and almost completely disappeared at the end of the study, 3 months post-injection (Figures 3E,F and S3E). As expected, a dose-dependent increase in the level of anti-hGAA IgG was measured in AAV-MT treated mice at 1 month after injection (Figures 3E,F and S3E). Importantly, in animals injected with the lower dose, of AAV-MT-LiMP vector the levels of circulating anti-hGAA IgG increased over time, whereas at the higher dose, anti-hGAA IgG decreased dramatically, possibly due to the residual expression of hGAA in liver.

Taken together, these results indicate a dose advantage in muscle correction in the use of a muscle specific AAV capsid when combined with the LiMP. They also reinforce the concept of residual liver expression as beneficial for the control of immune responses to the transgene.

2.2 | Muscle-specific targeting achieves long-term efficacy and functional rescue in neonate $Gaa^{-/-}$ mice

Neonate $Gaa^{-/-}$ mice were injected right after birth (post-natal day 0 to 2) with 1×10^{13} and 3×10^{13} vg/kg of AAV9 or AAV-MT vectors expressing hGAAco under the control of the LiMP. 6 months after vector injection, mice were sacrificed to compare the efficacy of the two vectors (Figure 4A). As expected, injection of neonate mice resulted in AAV vector genome dilution over time with low copies measured in liver at the end of the study, regardless of the treatment (0.42 ± 0.3 and 2.17 ± 0.8 for AAV9; 0.15 ± 0.2 and 0.46 ± 0.3 for AAV-MT, respectively at 1×10^{13} and 3×10^{13} vg/kg). Activity and expression of hGAA were observed in liver tissue in $Gaa^{-/-}$ mice treated with AAV9-LiMP vector at both doses (Figures 4B and S4A). Very low hGAA expression was observed also in the liver of animals treated with the AAV-MT-LiMP vector at the higher dose (Figure S4A). The measurement of circulating hGAA by Western blot confirmed the data of liver expression, with hGAA bands detected in the blood of AAV9-treated $Gaa^{-/-}$ mice and lower levels in the animals treated with AAV-MT at the dose of 3×10^{13} vg/kg (Figure S4B). GAA activity in heart was significantly higher in mice injected with AAV9 compared with AAV-MT (Figure 4C), and this correlated with higher VGCN measured in this tissue (Figure S5A). Despite the low GAA activity levels, complete correction of glycogen accumulation was observed in the hearts of all AAV-treated $Gaa^{-/-}$ mice, starting from the lower dose (Figure 4D,E), confirming that low levels of GAA are needed to clear glycogen from that tissue.[21] In skeletal muscle, increased GAA activity was measured in diaphragm, quadriceps, and triceps of

FIGURE 2 Specific muscle-targeting with AAV-MT results in improved glycogen clearance in skeletal muscle in adult Pompe mice. (A) Experimental design. 4-month-old $Gaa^{-/-}$ mice received a single injection of AAV9-LiMP-hGAAco or AAV-MT-LiMP-hGAAco at 1×10^{12} or 3×10^{12} vg/kg ($n = 4$ per group). PBS-injected $Gaa^{+/+}$ ($n = 4$) and $Gaa^{-/-}$ ($n = 4$) mice were used as controls. Red symbols indicate the timing of blood collection in all cohorts. (B) Analysis of GAA activity in muscles 3 months after vector injection. (C, D) Western blot analysis of hGAA in (C) quadriceps and (D) soleus. The quantification of hGAA protein band is plotted on the right. (E) Analysis of glycogen content in muscles 3 months after vector injection. Data are shown as mean ± SD. Statistical analysis; (B–E) One-way ANOVA with Tukey post hoc; * and $^{+}p < 0.05$, **, $^{++}$ and $^{\#\#}p < 0.01$, *** and $^{\#\#\#}p < 0.001$, ****, $^{++++}$ and $^{\#\#\#\#}p < 0.0001$. Statistical significance was reported as: $^{\#}$ versus $Gaa^{+/+}$, * versus $Gaa^{-/-}$, and with $^{+}$ versus the indicated group.

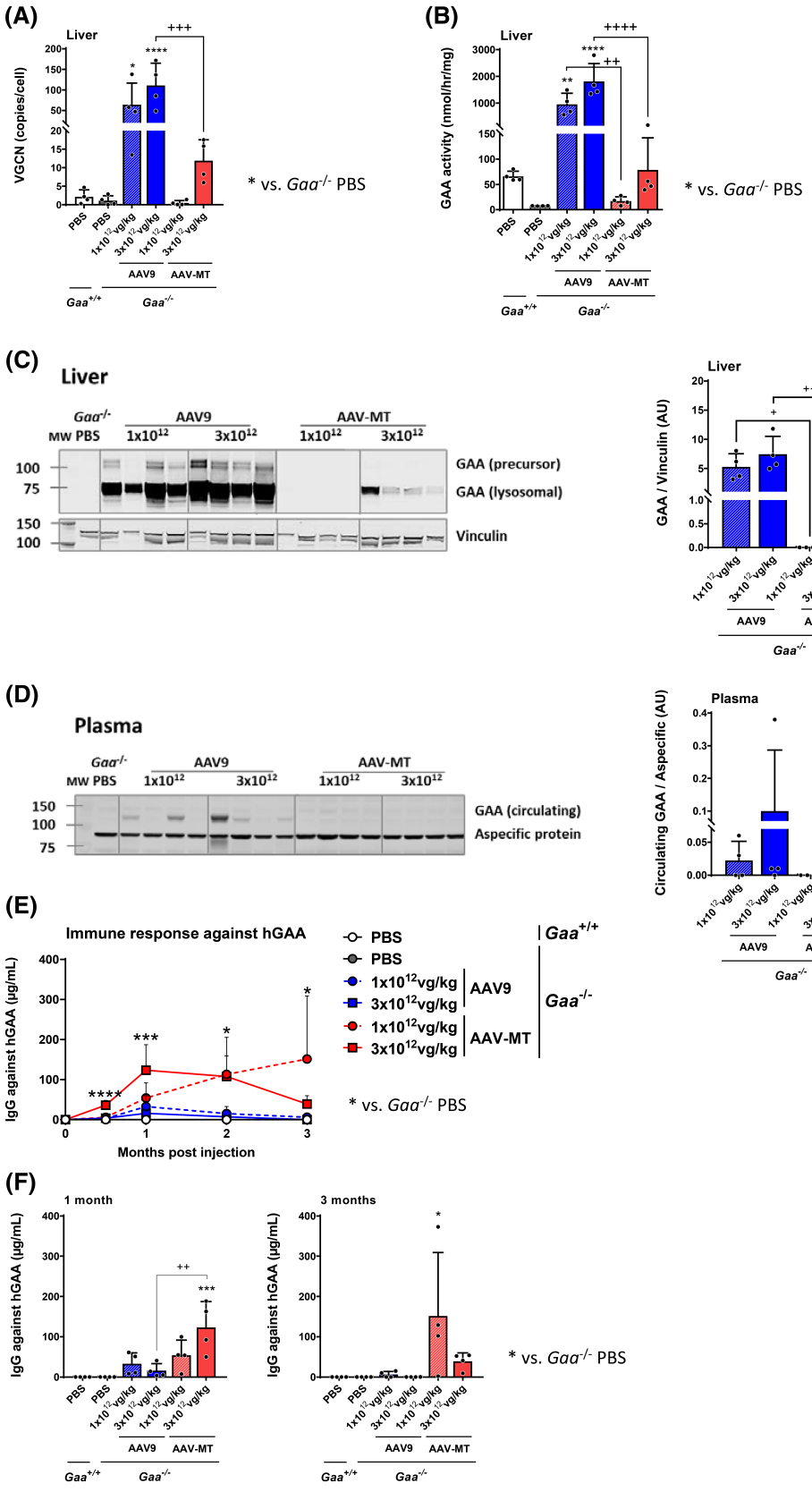

FIGURE 3 Residual liver transgene expression with AAV-MT combined with LiMP reduces anti-hGAA humoral response in adult Pompe mice. Four-month-old *Gaa*$^{-/-}$ mice were treated as described in Figure 2. (A, B) Analysis of vector genome copy number (VGCN) (A) and GAA activity (B) in liver at sacrifice. (C, D) Western blot analysis of hGAA in (C) liver and (D) blood. The quantification of the hGAA protein band is plotted on the right. (E) Circulating anti-hGAA IgG measured overtime. (F) Circulating anti-hGAA IgG measured at 1- and 3-months post-injection. Data are shown as mean ± SD. Statistical analysis; (A–F) One-way ANOVA with Tukey post hoc; * and $^{+}p < 0.05$, ** and $^{++}p < 0.01$, ***$p < 0.001$, **** and $^{++++}p < 0.0001$. Statistical significance was reported as: * versus *Gaa*$^{-/-}$, and with $^{+}$ versus the indicated group.

Gaa$^{-/-}$ mice injected with AAV-MT, which reached significance at the higher dose (Figure 4F). In line with these results, Western blot analysis showed enhanced hGAA expression in triceps of AAV-MT-treated mice, at 3×10^{13} vg/kg (Figure 4G). Increased GAA activity resulted in better glycogen clearance in all muscle groups

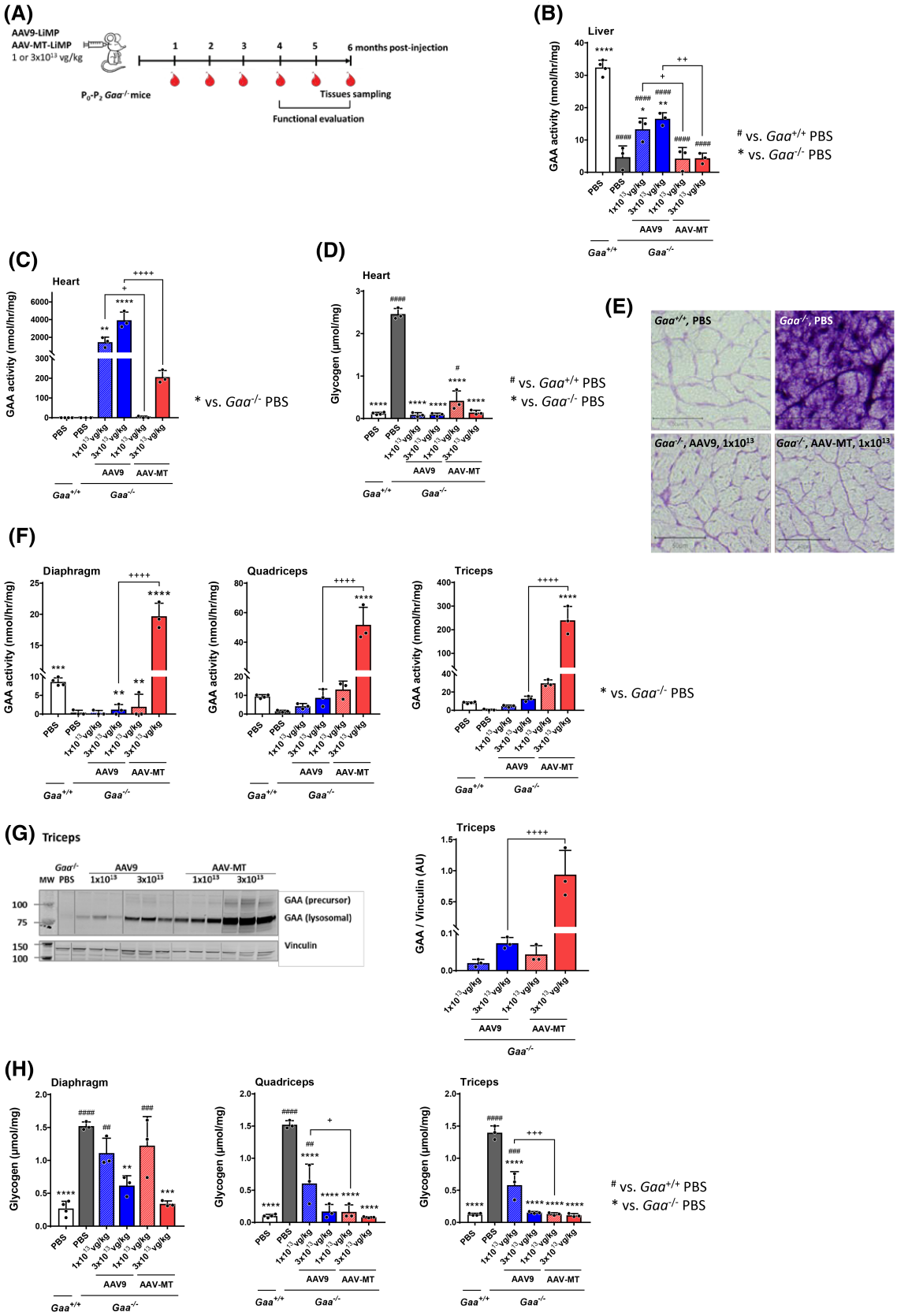

FIGURE 4 Legend on next page.

with a dose advantage for AAV-MT in quadriceps and triceps, and a tendency in diaphragm as measured by glycogen content (Figure 4H) and PAS staining (Figure S5B). Extensive glycogen clearance was also observed in soleus and EDL muscles. Importantly, at the lower dose, complete clearance of glycogen was observed in the soleus of *Gaa*$^{-/-}$ mice treated with AAV-MT, whereas rodents treated with AAV9 had levels comparable to those treated with PBS (Figure 5A). In EDL, complete glycogen clearance was measured in AAV-treated animals, all doses and vectors confounded (Figure 5A). PAS staining performed on these muscles confirmed the dose advantage of the AAV-MT vector, with better glycogen clearance in soleus at the higher dose (Figure 5B).

Assessment of functional improvements was performed to explore potential correction of cardiomegaly and improvement of muscle strength in AAV-treated *Gaa*$^{-/-}$ mice. Heart weight measurement showed a tendency to the increase in PBS-treated *Gaa*$^{-/-}$ mice although it did not reach significance, possibly due to the low number of animals considered. However, AAV-treated animals showed, in general, lower heart weight similar to PBS-treated *Gaa*$^{+/+}$ mice (Figure 5C). In line with the complete clearance of glycogen in skeletal muscle, rescue of muscle strength was observed at four and 6 months after AAV-MT treatment at the higher dose (Figure 5D). *Gaa*$^{-/-}$ mice treated with AAV9 vector at the lower dose were not rescued at both time points, thus confirming the dose advantage of muscle-specific targeting with AAV-MT vector.

Taken together, these data further support the use of muscle-specific targeting for the complete rescue of the Pompe phenotype in neonate *Gaa*$^{-/-}$ mice at doses relevant for the clinical translation of the approach.

3 | DISCUSSION

Since 1998, year of the first report of AAV gene therapy for Pompe disease,[51] a number of different approaches were reported to provide a curative treatment for this devastating disease.[52] Muscle being the primary tissue affected by the lack of GAA activity, its targeting by gene therapy was considered since the very beginning for the treatment of the disease and one clinical trial is ongoing using this approach (NCT04174105). As an alternative, the use of the liver to secrete the hGAA protein in the circulation has been proposed.[36,53] We previously showed that liver expression of a secretable hGAA effectively reduced the dose of AAV vector needed to clear glycogen from muscle cells and allowed for a complete rescue of the muscle function at very low AAV doses.[21–23] However, this approach is limited by liver growth during infancy and the resulting AAV vector dilution. On the other hand, muscle growth seems to have a lower effect on AAV genome dilution thus making muscle-directed gene therapy relevant for the treatment of classic infantile-onset Pompe disease (IOPD). One important limitation associated to muscle targeting with AAV vectors, is that the high doses necessary to achieve efficient transgene expression in muscle and the consequent liver overloading due to non-specific targeting are responsible for an important part of the severe adverse events reported in neuromuscular gene therapy.[54]

Here, we demonstrated the potential of the use of an AAV capsid grafted with an RGD-containing peptide to transduce muscle tissues in vivo while de-targeting the liver in a mouse model of PD. The efficacy of the new capsid was compared side-by-side at multiple doses with a state-of-the-art approach for the correction of neonate mice recently developed in our laboratory.[24] The combination of AAV-MT and LiMP resulted in a two-log increase in hGAA expression and enhanced glycogen clearance in different muscle groups when compared to an AAV9 vector bearing a muscle-specific promoter, SpC5-12. Importantly, due to the peculiar biodistribution profile of the AAV-MT, only residual expression of the transgene, comparable to that of SpC5-12, was observed despite the use of LiMP, a strong promoter in liver.[24] Extensive liver de-targeting with tremendously increased muscle targeting resulted in a robust humoral response to the transgene. To confirm the higher muscle targeting

FIGURE 4 Specific muscle-targeting with AAV-MT vector results in better skeletal muscle correction in neonate Pompe mice. (A) Experimental design. Neonate (P_0-P_2) *Gaa*$^{-/-}$ mice received a single injection of AAV9-LiMP-hGAAco or AAV-MT-LiMP-hGAAco at 1×10^{13} or 3×10^{13} vg/kg ($n = 3$ per group). Age-matched and sex-matched *Gaa*$^{+/+}$ and *Gaa*$^{-/-}$ littermates were used as controls ($n = 3$–4 per group). Red symbols indicate the timing of blood collection in all cohorts. (B) Analysis of GAA activity in the liver at sacrifice, 6 months after vector injection. (C, D) Analysis of GAA activity (C) and glycogen content (D) in heart at sacrifice. (E) Periodic Acid Schiff (PAS) staining performed in heart sections. (F) Analysis of GAA activity in muscles at sacrifice. (G) Western blot analysis of hGAA in triceps. The quantification of hGAA protein band is plotted on the right. (H) Analysis of glycogen content in muscles at sacrifice. Data are shown as mean ± SD. Statistical analysis; (B–H) One-way ANOVA with Tukey post hoc; $^{+}$ and $^{\#}p < 0.05$, ** and $^{\#\#}p < 0.01$, ***, $^{+++}$ and $^{\#\#\#}p < 0.001$, ****, $^{++++}$ and $^{\#\#\#\#}p < 0.0001$. Statistical significance was reported as: $^{\#}$ versus *Gaa*$^{+/+}$, * versus *Gaa*$^{-/-}$, and with $^{+}$ versus the indicated group.

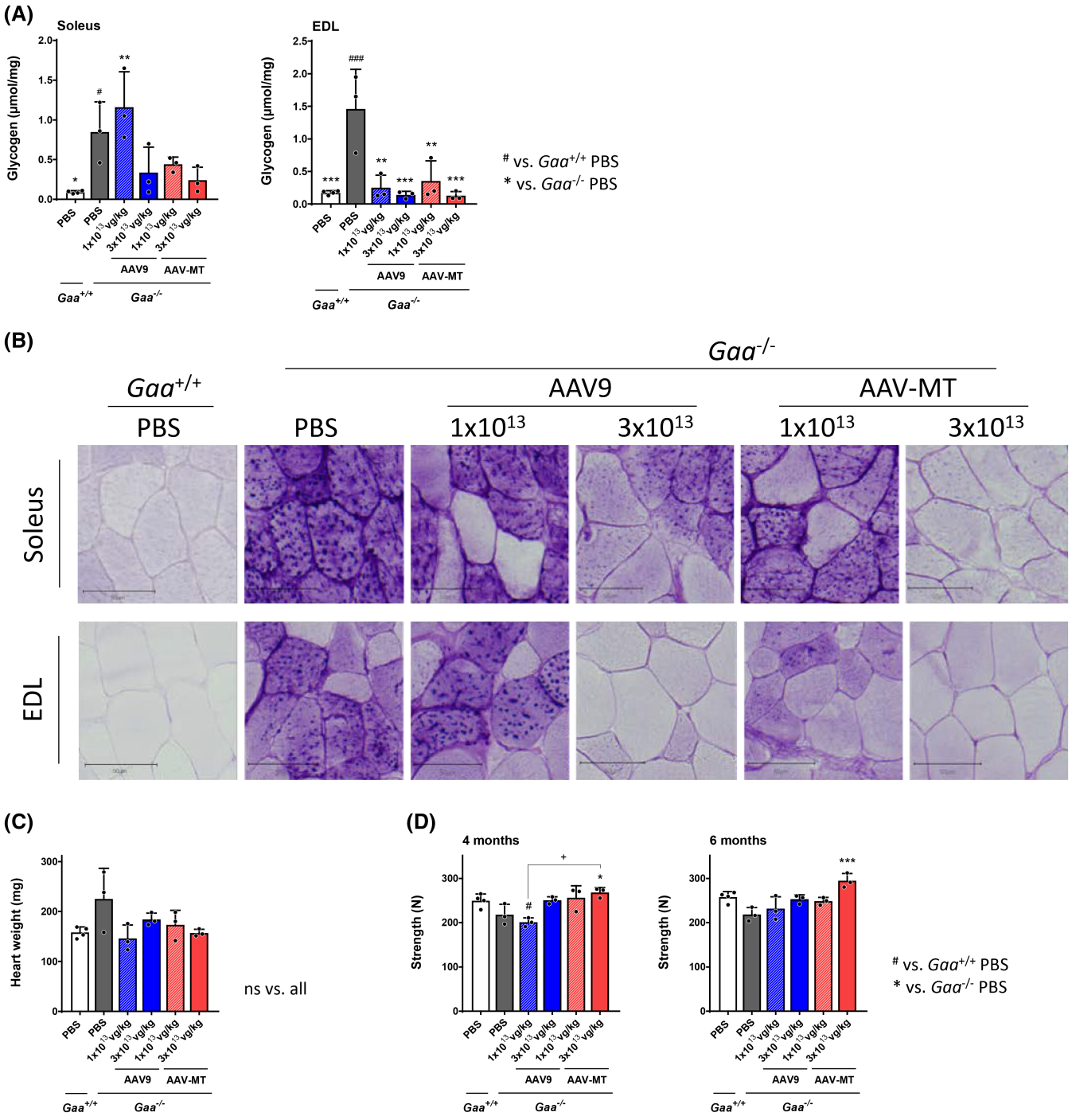

FIGURE 5 Muscle-specific targeting with AAV-MT vector achieves long-term efficacy in neonate Pompe mice. Neonate (P_0-P_2) *Gaa*$^{-/-}$ and *Gaa*$^{+/+}$ mice were treated as described in Figure 4. (A) Analysis of glycogen content in soleus and EDL at sacrifice. (B) Periodic Acid Schiff (PAS) staining performed in soleus and EDL sections. (C) Western blot analysis of hGAA in soleus. The quantification of hGAA protein band is plotted on the right. (D) Heart weight. (E) Grip strength measured 4 and 6 months after treatment. Data are shown as mean ± SD. Statistical analysis; (A–E) One-way ANOVA with Tukey post hoc; *, $^{+}$ and $^{\#}p < 0.05$, $^{**}p < 0.01$, *** and $^{\#\#\#}$ $p < 0.001$. Statistical significance was reported as: $^{\#}$ versus *Gaa*$^{+/+}$, * versus *Gaa*$^{-/-}$, and with $^{+}$ versus the indicated group.

and to further evaluate the humoral response against hGAA after muscle-specific gene transfer, we performed a multi-dose comparison in adult *Gaa*$^{-/-}$ mice. The use of an AAV9 vector in combination with LiMP was very efficient, the result of simultaneous muscle and liver targeting. Interestingly, despite the specific muscle targeting achieved by AAV-MT-LiMP, this vector demonstrated a clear dose-advantage when compared with AAV9-LiMP.

Intriguingly, although AAV-MT-treated animals showed greater humoral response to hGAA than AAV9-treated Pompe mice at 1 month, residual liver expression of hGAA, observed with the higher dose, resulted in reduced humoral response at the end of the study, 3 months after treatment. Most importantly, despite this apparently higher humoral response, specific muscle targeting achieved by AAV-MT-LiMP, demonstrated a clear dose-advantage in muscle correction when compared to AAV9-LiMP.

Finally, to demonstrate the full potential of muscle-specific targeting in PD, we performed an experiment in neonate animals, where the liver transduction achieved with AAV9 is diluted over time, thus allowing a direct comparison of muscle transduction with little to no circulating hGAA. Despite the fast liver growth, and due to the high doses needed to target the muscle in neonate animals, liver expression (corresponding to 50% of the activity measured in $Gaa^{+/+}$ animals) was reported in AAV9-injected animals, whereas it was almost absent in AAV-MT treated animals, in particular at the lower dose. Despite this bias toward AAV9, the data in neonate $Gaa^{-/-}$ mice indicate, as observed in adult animals, a dose advantage for the AAV-MT-LiMP vector. Indeed, 6 months after treatment, our results showed almost complete clearance of glycogen in multiple muscle groups, starting from the lower dose of AAV-MT. Moreover, improved muscle strength at both four and six months after vector injection in $Gaa^{-/-}$ animals treated with 3×10^{13} vg/kg was observed.

One important open question in the use of AAV gene therapy for PD is the development of anti-hGAA antibodies in IOPD patients when they are CRIM. Although we demonstrated that even low levels of hGAA liver expression could reduce the humoral response to the transgene, the robustness of the induction of peripheral tolerance after liver gene transfer in humans is still questioned. However, protocols for tolerance induction are being developed for IOPD patients[55] and, in combination with muscle-directed gene therapy, they may be able to provide an alternative treatment to ERT in this patients' population.

Noteworthy, the treatment in neonate $Gaa^{-/-}$ mice required doses of vectors almost 10 times higher than the treatment of adult mice to achieve complete correction of the muscle phenotype 6 months after vector injection. Although this could be related primarily to a potential difference in efficacy of gene transfer in neonates compared with adults, one intriguing hypothesis is that during growth, the muscle mass increase may somehow dilute the vector although with a transgene loss less spectacular than that reported after liver growth.[56–60] If this growth-dependent vector dilution in muscle is confirmed and given the formation of high titer anti-AAV antibodies after the injection of AAV vectors, strategies may be needed to be able to cope with vector re-administration. Recently, the use of IdeS[61–63] or AAV vector-specific plasmapheresis[64,65] were proposed by different groups as clinically-relevant approaches to reduce circulating anti-AAV antibodies and allow for vector re-administration.

In our work, we used a muscle-tropic, liver de-targeted AAV capsid to normalize glycogen accumulation and rescue muscle strength in a mouse model of PD. However, in the last years, the efforts of researchers in the characterization of the disease manifestation in IOPD treated with Myozyme, reveal the emergence of white matter abnormality that may be associated with cognitive function impairment.[66–68] Central nervous system targeting by the new, RGD-based, muscle tropic capsids was not previously reported and, it is likely that the RGDLGLS peptide grafted will not confer better biodistribution to this tissue. Another potential limitation of the current study is related to the poor translatability of AAV vector biodistribution across species. Although the main objective of the present work was to demonstrate the advantages of the use of AAV/promoter combination to tailor transgene expression to the disease, confirmation of these results in large animal preclinical models (e.g., primates[23] or Pompe dogs[69]) may be needed to further support clinical development.

To conclude, AAV vectors with enhanced muscle targeting and improved liver de-targeting represent an alternative to the existing gene therapy approaches for IOPD. If these results are confirmed in large animal models, AAV-MT may represent a valid alternative to the existing AAV vectors to reduce liver overload and the high vector doses accounting for many of the serious adverse events recently reported in AAV gene therapy for neuromuscular diseases. Combination of this approach with emerging methods to control the immunogenicity against the vector and the transgene is required to efficiently treat PD while ensuring safety.

4 | MATERIALS AND METHODS

4.1 | Plasmids

The hGAA transgene expression cassette used was already described in Reference 24 and was used to express a codon-optimized version of the native human GAA (hGAAco) as in Reference 21.

4.2 | AAV vector production

AAV-MT-LiMP-GAAco and AAV9-LiMP-GAAco vectors were produced by an adenovirus-free transient tri-

transfection method of HEK 293 cells in suspension and purified by affinity chromatography. Titers of AAV vectors were determined using qPCR and all vector preparations used in the studies were quantified side by side.

4.3 | Mouse model

Comparative efficacy studies were performed in male *Gaa* knockout mice ($Gaa^{-/-}$), purchased from The Jackson Laboratory (B6;129-$Gaa^{tm1Rabn/J}$, stock number 004154, 6neo) and originally generated by Raben et al.[70] Littermate male mice were used, either affected ($Gaa^{-/-}$) or healthy ($Gaa^{+/+}$). We have reported the phenotype of males $Gaa^{-/-}$ versus $Gaa^{+/+}$ from our colonies in previous work.[21]

4.4 | In vivo studies in mice

In vivo studies were performed in compliance with all relevant ethical regulations for animal testing and research. Notably, they were performed according to the French and European legislation on animal care and experimentation (2010/63/EU) and approved by Genethon's ethical committee. In all mouse studies, animals were randomly assigned to treatment groups. To minimize potential bias during functional assessments in mice, operators were blinded to the study design. Operators in charge of sample analysis were blinded to study design.

4.4.1 | Experiments in adult mice

Treatments with AAV vectors were performed in male $Gaa^{-/-}$ mice of 4 months of age, that received either intravenous injection of vehicle (PBS), AAV9-LiMP-GAAco or AAV-MT-LiMP-GAAco. Four animals per group were injected via tail vein infusion with 1×10^{12} or 3×10^{12} vg/kg of vector (in a volume of 200 μL). Age-matched and sex-matched $Gaa^{+/+}$ littermates were used as healthy controls in the studies.

4.4.2 | Experiment in neonate mice

Male $Gaa^{-/-}$ mice from birth to 2 days of age were treated either with PBS, AAV9-LiMP-GAAco or AAV-MT-LiMP-GAAco vectors. Three animals per group were injected via tail vein infusion with 1×10^{13} or 3×10^{13} vg/kg of vector (in a volume of 20 μL). Age-matched and sex-matched $Gaa^{+/+}$ littermates were used as healthy controls in the studies.

4.5 | Blood GAA activity and anti-hGAA IgG measurement

Blood samples were collected by retro-orbital sampling into heparinized capillary tubes and mixed with 3.8% wt/vol sodium citrate, followed by plasma isolation. GAA activity measurement was performed as already described.[21] The concentration of anti-hGAA IgG antibodies in mouse plasma was determined by enzyme-linked immunosorbent assay (ELISA).[21]

4.6 | Tissue GAA activity and Western blot analyses

Snap-frozen tissues were homogenized in UltraPure DNase/RNase-free water (Thermo Fisher Scientific, Waltham, MA) with FastPrep lysis tubes (MP Biomedicals, OH), followed by centrifugation 20 min at 10 000*g* to collect the supernatant. Protein content in lysates was quantified by BCA Protein Assay (Thermo Fisher Scientific). GAA activity measurement was performed as already described.[21] SDS-page electrophoresis was performed with NuPAGE 4%–12% Bis-Tris protein gels (Life Technologies, Carlsbad, CA). After transfer, the membrane was blocked with Odyssey buffer (Li-Cor Biosciences) and incubated with an anti-hGAA antibody (rabbit monoclonal, clone EPR4716[2], Abcam) and anti-Vinculin (mouse monoclonal, clone V9131, Sigma-Aldrich). Membrane was then washed and incubated with the appropriate secondary antibody (LI-COR Biosciences) and visualized with the Odyssey imaging system (Li-Cor Biosciences). Densitometry analysis was conducted using Image Studio Lite (Li-Cor Biosciences) version 4.0. The quantification of the hGAA bands in mouse tissues was normalized using housekeeping Vinculin protein bands. Protein level was reported in units of arbitrary unity (AU).

4.7 | Glycogen content measurement

Tissue homogenates samples were prepared as described for the analysis of GAA activity. Glycogen assay was performed as already described.[21]

4.8 | Vector genome copy number

Vector genome copies in mice were determined by qPCR on total tissue DNA. Total DNA was extracted from tissues homogenates using NucleoMag Pathogen (Macherey-Nagel, Hoerdt, France) extraction method

according to manufacturer's instructions. The number of vector copies per diploid genome was determined using primers to amplify the GAAco transgene sequence (forward: 5′-AGATACGCCGGACATTGGACTG-3′; reverse: 5′-GTTCAATCTGCTGGGCGTGC-3′; probe: 5′-GTGTGGTCCTCTTGGGAGC-3′). The number of vector copies was normalized by the copies of the *titin* gene, which was used as an internal control for each sample (forward: 5′-AAAACGAGCAGTGACGTGAGC-3′; reverse: 5′-TTCAGTCATGCTGCTAGCGC-3′; probe, 5′-TGCACGGAAGCGTCTCGTCTCAGT-3′). Data were expressed as vector genome copies per diploid genome.

4.9 | Histology and staining

Immediately after euthanasia, muscles were snap-frozen in isopentane (−160°C) previously chilled in liquid nitrogen. Serial 8 mm cross-sections were cut in a Leica CM3050 S cryostat (Leica Biosystems, Wetzlar, Germany). To minimize sampling error, two or three sections of each specimen were obtained and stained with periodic acid-Schiff (PAS) according to standard procedures. Muscle images were acquired using an Axioscan slide scanner (ZEISS, Munich, Germany), using a plan-apochromat ×10 magnitude 0.45 NA objective.

4.10 | Grip test

Muscle strength was assessed using a grip strength meter (Columbus Instruments, Columbus, OH).[20] Briefly, mice were lifted by the tail to the same height of the grip strength meter grid. Mice were then moved horizontally until they were within reach. Four-limb grip was inspected visually to confirm the symmetry and the tight grip. Mice were then gently pulled away from the grid until the grasp was released. The Grip strength meter recorded the value. Three independent measures were performed for each mouse. Mean values of three independent measures expressed in Newton were reported.

4.11 | Statistical analysis

All data shown in the present manuscript are expressed as mean ± standard deviation (SD). GraphPad Prism 7.0 software (GraphPad Software, San Diego, CA) was used for statistical analyses. p-value < 0.05 was considered significant. The number of sampled units (n), upon which we reported statistics is the single animal. Parametric tests were used for data having a normal distribution with $\alpha = 0.05$. One-way ANOVA with Tukey's post hoc correction was used for comparisons of one variable between more than two groups. All statistical tests were performed two-sided. The statistical analysis performed for each dataset is indicated in the figure legends.

AUTHOR CONTRIBUTIONS

P. Sellier, F. Collaud, and G. Ronzitti performed or directed experimental activities and contributed significantly to experimental design. F. Mingozzi, G. Ronzitti, P. Vidal, I. Richard, and E. Gicquel, designed the AAV-MT capsid. B. Bertin performed AAV vectors production. P. Sellier performed experiments and data analysis. P. Sellier, F. Collaud, and G. Ronzitti wrote the manuscript. F. Mingozzi and D. A. Gross provided insights into the disease pathophysiology, AAV vector technology and immunology. E. Bertil-Froidevaux, C. Georger, L. van Wittenberghe, A. Miranda, and N. Daniele contributed to experimental activities. All authors approved the final manuscript.

ACKNOWLEDGMENTS

This work was supported by Genethon and the French Muscular Dystrophy Association (AFM). D. A. Gross was supported by a grant from the SPARK Competitive Research Grant Program on Pompe disease. We thank Nicolas Guerchet and Guillaume Tanniou for their help with the functional testing; the Genethon Histology Core for technical help with histology. We also thank the Imaging and Cytometry Core Facility of Genethon.

CONFLICT OF INTEREST STATEMENT

F. Collaud, F. Mingozzi, and G. Ronzitti are inventors in patents applications concerning the treatment of Pompe disease by AAV licensed to Spark Therapeutics (WO2018046774, WO2018046775, WO2018046775). F. Mingozzi, G. Ronzitti, P. Vidal, I. Richard, and E. Gicquel are authors in patents related to AAV capsid development. F. Mingozzi is a current employee and equity holder of Spark Therapeutics, Inc., a Roche company. All other authors declare no conflict of interest.

DATA AVAILABILITY STATEMENT

All data presented in the manuscript are available upon reasonable request.

ETHICS STATEMENT

All institutional and national guidelines for the care and use of laboratory animals were followed. This article does not contain any studies with human or animal subjects performed by any of the authors.

ORCID

G. Ronzitti https://orcid.org/0000-0002-9184-0210

REFERENCES

1. van der Ploeg AT, Reuser AJ. Pompe's disease. *Lancet*. 2008; 372(9646):1342-1353.
2. Sarah B, Giovanna B, Emanuela K, Nadi N, Josè V, Alberto P. Clinical efficacy of the enzyme replacement therapy in patients with late-onset Pompe disease: a systematic review and a meta-analysis. *J Neurol*. 2022;269(2):733-741.
3. Masat E, Laforêt P, de Antonio M, et al. Long-term exposure to Myozyme results in a decrease of anti-drug antibodies in late-onset Pompe disease patients. *Sci Rep*. 2016;6:36182.
4. Patel TT, Banugaria SG, Case LE, Wenninger S, Schoser B, Kishnani PS. The impact of antibodies in late-onset Pompe disease: a case series and literature review. *Mol Genet Metab*. 2012;106(3):301-309.
5. Amalfitano A, Bengur AR, Morse RP, et al. Recombinant human acid alpha-glucosidase enzyme therapy for infantile glycogen storage disease type II: results of a phase I/II clinical trial. *Genet Med*. 2001;3(2):132-138.
6. Kishnani PS, Corzo D, Nicolino M, et al. Recombinant human acid [alpha]-glucosidase: major clinical benefits in infantile-onset Pompe disease. *Neurology*. 2007;68(2):99-109.
7. Nicolino M, Byrne B, Wraith JE, et al. Clinical outcomes after long-term treatment with alglucosidase alfa in infants and children with advanced Pompe disease. *Genet Med*. 2009;11(3): 210-219.
8. Chien Y-H, Lee NC, Chen CA, et al. Long-term prognosis of patients with infantile-onset Pompe disease diagnosed by newborn screening and treated since birth. *J Pediatr*. 2015;166(4): 985-991. e2.
9. Prater SN, Banugaria SG, DeArmey SM, et al. The emerging phenotype of long-term survivors with infantile Pompe disease. *Genet Med*. 2012;14(9):800-810.
10. Prater SN, Patel TT, Buckley AF, et al. Skeletal muscle pathology of infantile Pompe disease during long-term enzyme replacement therapy. *Orphanet J Rare Dis*. 2013;8(1):1-12.
11. Chien Y-H, Lee NC, Thurberg BL, et al. Pompe disease in infants: improving the prognosis by newborn screening and early treatment. *Pediatrics*. 2009;124(6):e1116-e1125.
12. Kishnani PS, Hwu WL, Mandel H, et al. A retrospective, multinational, multicenter study on the natural history of infantile-onset Pompe disease. *J Pediatr*. 2006;148(5):671-676. e2.
13. Matsuoka T, Miwa Y, Tajika M, et al. Divergent clinical outcomes of alpha-glucosidase enzyme replacement therapy in two siblings with infantile-onset Pompe disease treated in the symptomatic or pre-symptomatic state. *Mol Genet Metab Rep*. 2016;9:98-105.
14. Kishnani PS, Goldenberg PC, DeArmey SL, et al. Cross-reactive immunologic material status affects treatment outcomes in Pompe disease infants. *Mol Genet Metab*. 2010;99(1):26-33.
15. Desai AK, Kazi ZB, Kishnani PS. Cross-reactive immunologic material positive infantile Pompe disease: characterization of immune responses in patient treated with enzyme replacement therapy. *Mol Genet Metab*. 2016;2(117):S41.
16. Banugaria SG, Prater SN, Ng YK, et al. The impact of antibodies on clinical outcomes in diseases treated with therapeutic protein: lessons learned from infantile Pompe disease. *Genet Med*. 2011;13(8):729-736.
17. Unnisa Z, Yoon JK, Schindler JW, Mason C, van Til NP. Gene therapy developments for Pompe disease. *Biomedicine*. 2022; 10(2):302.
18. Franco LM, Sun B, Yang X, et al. Evasion of immune responses to introduced human acid alpha-glucosidase by liver-restricted expression in glycogen storage disease type II. *Mol Ther*. 2005; 12(5):876-884.
19. Sun B, Kulis MD, Young SP, et al. Immunomodulatory gene therapy prevents antibody formation and lethal hypersensitivity reactions in murine pompe disease. *Mol Ther*. 2010;18(2):353-360.
20. Zhang P, Sun B, Osada T, et al. Immunodominant liver-specific expression suppresses transgene-directed immune responses in murine pompe disease. *Hum Gene Ther*. 2012;23(5):460-472.
21. Puzzo F, Colella P, Biferi MG, et al. Rescue of Pompe disease in mice by AAV-mediated liver delivery of secretable acid alpha-glucosidase. *Sci Transl Med*. 2017;9(418):eaam6375.
22. Cagin U, Puzzo F, Gomez MJ, et al. Rescue of advanced Pompe disease in mice with hepatic expression of secretable acid α-glucosidase. *Mol Ther*. 2020;28:2056-2072.
23. Costa-Verdera H, Collaud F, Riling CR, et al. Hepatic expression of GAA results in enhanced enzyme bioavailability in mice and non-human primates. *Nat Commun*. 2021;12(1):6393.
24. Colella P, Sellier P, Costa Verdera H, et al. AAV gene transfer with tandem promoter design prevents anti-transgene immunity and provides persistent efficacy in neonate Pompe mice. *Mol Ther Methods Clin Dev*. 2019;12:85-101.
25. Han SO, Ronzitti G, Arnson B, et al. Low-dose liver-targeted gene therapy for Pompe disease enhances therapeutic efficacy of ERT via immune tolerance induction. *Mol Ther Methods Clin Dev*. 2017;4:126-136.
26. Bortolussi G, Zentillin L, Vaníkova J, et al. Life-long correction of hyperbilirubinemia with a neonatal liver-specific AAV-mediated gene transfer in a lethal mouse model of Crigler-Najjar syndrome. *Hum Gene Ther*. 2014;25(9):844-855.
27. Cresawn KO, Fraites TJ Jr, Wasserfall C, et al. Impact of humoral immune response on distribution and efficacy of recombinant adeno-associated virus-derived acid alpha-glucosidase in a model of glycogen storage disease type II. *Hum Gene Ther*. 2005;16(1):68-80.
28. Falk DJ, Mah CS, Soustek MS, et al. Intrapleural administration of AAV9 improves neural and cardiorespiratory function in Pompe disease. *Mol Ther*. 2013;21(9):1661-1667.
29. Falk DJ, Soustek MS, Todd AG, et al. Comparative impact of AAV and enzyme replacement therapy on respiratory and cardiac function in adult Pompe mice. *Mol Ther Methods Clin Dev*. 2015;2:15007.
30. Fraites TJ Jr, Schleissing MR, Shanely RA, et al. Correction of the enzymatic and functional deficits in a model of Pompe disease using adeno-associated virus vectors. *Mol Ther*. 2002;5(5 Pt 1):571-578.
31. Mah C, Cresawn KO, Fraites TJ Jr, et al. Sustained correction of glycogen storage disease type II using adeno-associated virus serotype 1 vectors. *Gene Ther*. 2005;12(18):1405-1409.
32. Mah C, Pacak CA, Cresawn KO, et al. Physiological correction of Pompe disease by systemic delivery of adeno-associated virus serotype 1 vectors. *Mol Ther*. 2007;15(3):501-507.
33. Mah CS, Falk DJ, Germain SA, et al. Gel-mediated delivery of AAV1 vectors corrects ventilatory function in Pompe mice with established disease. *Mol Ther*. 2010;18(3):502-510.
34. Rucker M, Fraites TJ Jr, Porvasnik SL, et al. Rescue of enzyme deficiency in embryonic diaphragm in a mouse model of metabolic myopathy: Pompe disease. *Development*. 2004;131(12): 3007-3019.

35. Sun B, Zhang H, Franco LM, et al. Correction of glycogen storage disease type II by an adeno-associated virus vector containing a muscle-specific promoter. *Mol Ther*. 2005;11(6):889-898.
36. Sun B, Zhang H, Franco LM, et al. Efficacy of an adeno-associated virus 8-pseudotyped vector in glycogen storage disease type II. *Mol Ther*. 2005;11(1):57-65.
37. Todd AG, McElroy JA, Grange RW, et al. Correcting neuromuscular deficits with gene therapy in Pompe disease. *Ann Neurol*. 2015;78(2):222-234.
38. Childers MK, Joubert R, Poulard K, et al. Gene therapy prolongs survival and restores function in murine and canine models of myotubular myopathy. *Sci Transl Med*. 2014;6(220):220ra10.
39. Le Guiner C, Servais L, Montus M, et al. Long-term microdystrophin gene therapy is effective in a canine model of Duchenne muscular dystrophy. *Nat Commun*. 2017;8:16105.
40. Mack DL, Poulard K, Goddard MA, et al. Systemic AAV8-mediated gene therapy drives whole-body correction of myotubular myopathy in dogs. *Mol Ther*. 2017;25(4):839-854.
41. Rapti K, Grimm D. Adeno-associated viruses (AAV) and host immunity – a race between the hare and the hedgehog. *Front Immunol*. 2021;12:753467.
42. Sun B, Li S, Bird A, et al. Antibody formation and mannose-6-phosphate receptor expression impact the efficacy of muscle-specific transgene expression in murine Pompe disease. *J Gene Med*. 2010;12(11):881-891.
43. El Andari J, Renaud-Gabardos E, Tulalamba W, et al. Semirational bioengineering of AAV vectors with increased potency and specificity for systemic gene therapy of muscle disorders. *Sci Adv*. 2022;8(38):eabn4704.
44. Tabebordbar M, Lagerborg KA, Stanton A, et al. Directed evolution of a family of AAV capsid variants enabling potent muscle-directed gene delivery across species. *Cell*. 2021;184(19):4919-4938 e22.
45. Weinmann J, Weis S, Sippel J, et al. Identification of a myotropic AAV by massively parallel in vivo evaluation of barcoded capsid variants. *Nat Commun*. 2020;11(1):5432.
46. Richard I, Gicquel E, Mingozzi F, Ronzitti G, Vidal P. *Hybrid recombinant adeno-associated virus serotype between AAV9 and AAVrh74 with reduced liver tropism*. Patent WO/2019/193119.
47. Ronzitti G, Vidal P, Mingozzi F. *Peptide-modified hybrid recombinant adeno-associated virus serotype between AAV9 AND AAVrh74 with reduced liver tropism and increased muscle transduction*. Patent WO/2020/200499.
48. Poupiot J, Costa Verdera H, Hardet R, et al. Role of regulatory T cell and effector T cell exhaustion in liver-mediated transgene tolerance in muscle. *Mol Ther Methods Clin Dev*. 2019;15:83-100.
49. Bartolo L, Li Chung Tong S, Chappert P, et al. Dual muscle-liver transduction imposes immune tolerance for muscle transgene engraftment despite preexisting immunity. *JCI Insight*. 2019;4(11):e127008.
50. Pulicherla N, Shen S, Yadav S, et al. Engineering liver-detargeted AAV9 vectors for cardiac and musculoskeletal gene transfer. *Mol Ther*. 2011;19(6):1070-1078.
51. Tsujino S, Kinoshita N, Tashiro T, et al. Adenovirus-mediated transfer of human acid maltase gene reduces glycogen accumulation in skeletal muscle of Japanese quail with acid maltase deficiency. *Hum Gene Ther*. 1998;9(11):1609-1616.
52. Ronzitti G, Collaud F, Laforet P, Mingozzi F. Progress and challenges of gene therapy for Pompe disease. *Ann Transl Med*. 2019;7(13):287.
53. Sun B, Zhang H, Benjamin DK Jr, et al. Enhanced efficacy of an AAV vector encoding chimeric, highly secreted acid alpha-glucosidase in glycogen storage disease type II. *Mol Ther*. 2006;14(6):822-830.
54. High-dose AAV gene therapy deaths. High-dose AAV gene therapy deaths. *Nat Biotechnol*. 2020;38(8):910.
55. Desai AK, Li C, Rosenberg AS, Kishnani PS. Immunological challenges and approaches to immunomodulation in Pompe disease: a literature review. *Ann Transl Med*. 2019;7(13):285.
56. Nakai H, Yant SR, Storm TA, Fuess S, Meuse L, Kay MA. Extrachromosomal recombinant adeno-associated virus vector genomes are primarily responsible for stable liver transduction in vivo. *J Virol*. 2001;75(15):6969-6976.
57. Wang L, Bell P, Lin J, Calcedo R, Tarantal AF, Wilson JM. AAV8-mediated hepatic gene transfer in infant rhesus monkeys (Macaca mulatta). *Mol Ther*. 2011;19(11):2012-2020.
58. Cunningham SC, Dane AP, Spinoulas A, Alexander IE. Gene delivery to the juvenile mouse liver using AAV2/8 vectors. *Mol Ther*. 2008;16(6):1081-1088.
59. Bortolussi G, Zentilin L, Baj G, et al. Rescue of bilirubin-induced neonatal lethality in a mouse model of Crigler-Najjar syndrome type I by AAV9-mediated gene transfer. *FASEB J*. 2012;26(3):1052-1063.
60. Mingozzi F, High KA. Therapeutic in vivo gene transfer for genetic disease using AAV: progress and challenges. *Nat Rev Genet*. 2011;12(5):341-355.
61. Leborgne C, Barbon E, Alexander JM. IgG-cleaving endopeptidase enables in vivo gene therapy in the presence of anti-AAV neutralizing antibodies. *Nat Med*. 2020;26:1096-1101.
62. Elmore ZC, Oh DK, Simon KE, Fanous MM, Asokan A. Rescuing AAV gene transfer from neutralizing antibodies with an IgG-degrading enzyme. *JCI Insight*. 2020;5(19):e139881.
63. Ros-Ganan I, Hommel M, Trigueros-Motos L, et al. Optimising the IgG-degrading enzyme treatment regimen for enhanced adeno-associated virus transduction in the presence of neutralising antibodies. *Clin Transl Immunol*. 2022;11(2):e1375.
64. Bertin B, Veron P, Leborgne C, et al. Capsid-specific removal of circulating antibodies to adeno-associated virus vectors. *Sci Rep*. 2020;10(1):1-11.
65. Orlowski A, Katz MG, Gubara SM, Fargnoli AS, Fish KM, Weber T. Successful transduction with AAV vectors after selective depletion of anti-AAV antibodies by immunoadsorption. *Mol Ther Methods Clin Dev*. 2020;16:192-203.
66. Ebbink BJ, Poelman E, Aarsen FK, et al. Classic infantile Pompe patients approaching adulthood: a cohort study on consequences for the brain. *Dev Med Child Neurol*. 2018;60(6):579-586.
67. Korlimarla A, Spiridigliozzi GA, Crisp K, et al. Novel approaches to quantify CNS involvement in children with Pompe disease. *Neurology*. 2020;95(6):e718-e732.
68. McIntosh PT, Hobson-Webb LD, Kazi ZB, et al. Neuroimaging findings in infantile Pompe patients treated with enzyme replacement therapy. *Mol Genet Metab*. 2018;123(2):85-91.
69. Seppala EH, Reuser AJ, Lohi H. A nonsense mutation in the acid alpha-glucosidase gene causes Pompe disease in Finnish and Swedish Lapphunds. *PLoS One*. 2013;8(2):e56825.

70. Raben N, Nagaraju K, Lee E, et al. Targeted disruption of the acid alpha-glucosidase gene in mice causes an illness with critical features of both infantile and adult human glycogen storage disease type II. *J Biol Chem*. 1998;273(30):19086-19092.

SUPPORTING INFORMATION

Additional supporting information can be found online in the Supporting Information section at the end of this article.

How to cite this article: Sellier P, Vidal P, Bertin B, et al. Muscle-specific, liver-detargeted adeno-associated virus gene therapy rescues Pompe phenotype in adult and neonate *Gaa*$^{-/-}$ mice. *J Inherit Metab Dis*. 2023;1-16. doi:10.1002/jimd.12625